



FLUID FLOW STUDY IN VARIOUS SHAPES AND SIZES OF HORIZONTAL AXIS SEA CURRENT TURBINE

Wulfilla M. Rumaherang*, Jonny Latuny

Department of Mechanical Engineering, Faculty of Engineering, Universitas Pattimura, Indonesia



Abstract

The ducted tidal turbine models have been developed to utilize the conversion of the kinetic energy on ocean currents. The research in refining the turbine characteristics has been carried out by modifying the turbine's shape and size. This study investigated flow characteristics in the meridional section of five ducted turbines models for seawater flow with velocity $U_0 = 1.5$ m/s. The ducted turbine design and construction have five different impeller house diameters and fixed inlet and outlet diameters. The potential energy flow theory and experimental data are used to analyze the flow characteristics of the model. The results show that flow velocity in the x-direction at the inlet and outlet cross-section is getting smaller, reducing the impeller house cross section. Each impeller house size reduction increases the flow speed in the impeller house cross-section and also pressure on all other cross-sections tested. In the inlet area, the increased pressure indicates a decrease in speed flow and discharge coefficient value. The discharge coefficient value decreases from $C_D = 0.9$ at the diameter ratio of $dr = 1$ to $C_D = 0.56$ at the diameter ratio of $dr = 0.375$. The maximum value of power coefficient was determined at $dr = 0.61 \div 0.73$ or $dr = 0.69$ which is equivalent to average internal flow velocity $V_r = 2.0 \div 2.6$ m/s and the static pressure $p_s = 97.1 \div 94.4$ kPa. At the ratio value of $D_0/D_2 = 0.83$, the optimal diameter ratio $dr_{opt} = 0.61 \div 0.73$ is in line with the duct model of case 3 and case 4, but it may be determined solely as for case 4.

This is an open access article under the [CC BY-NC](#) license



Keywords:

Diameter ratio;
Ducted turbine;
Flow characteristics;

Article History:

Received: October 19, 2020
Revised: April 11, 2021
Accepted: May 18, 2021
Published: August 10, 2021

Corresponding Author:

Wulfilla M. Rumaherang
Department of Mechanical
Engineering, Faculty of
Engineering, Universitas
Pattimura, Indonesia
Email:
max.rumaherang@fatek.unpatti.ac.id

INTRODUCTION

The role of energy in the economic development in all nations is indispensable. Hence sectors such as industry, transportation, trade, and communication will be posing massive challenges without the availability of energy sources such as electricity. Unfortunately, many regions, especially in developing nations, are posing the problem of electricity sources. The topography and geography characteristics and the condition of a dispersed population in a region are some main obstacles for an effort to distribute energy. The power generation based on the current river turbine is one of the clean, decentralized renewable technologies that can supply energy to the regions where the conditions of the

topography, geography, and population have become the obstacles for the generation and distribution of energy.

Seawater currents in the straits between small islands in Maluku have speed flows reaching 2.5 m/s. Therefore, it is one of the potential energy resources to convert into electrical energy [1]. One of the ocean's current technologies is the horizontal ducted turbine [2][3], which is currently mostly in its development studies within the construction of tidal power equipment [3].

The turbine performance optimization studies are still conducted through the design and testing of various models, shapes, and sizes. The study is conducted to increase power at smaller rotor sizes, rotating at faster

rotational speeds to support gearbox and generator operations, reducing the cost per kilowatt generated on tidal power [4].

Tidal turbine performance is a relationship of power, rotation, and thrust parameters as a function of the free speed of ocean currents. The performance of the ducted tidal turbine model is closely dependent on the fluid flow properties through each cross-section whose principle is similar to the flow on the shrouded wind turbines, which its experimental studies have been carried out by others [5, 6, 7, 8].

The angle of outlet diffuser extraction influences the fluid flow characteristics through the cross-section of the shrouded wind turbine [6]. In addition, the flow velocity can be amplified through ducted shape design [9], diffuser design [10], and flow analysis in ducted turbines [11].

The coefficient of performance of micro wind turbines has increased by around 60% and the speed ratio has increased by 33% by adding a simple cone diffuser. This value is a result of the comparison to turbines without shrouded structures. Flow analysis is carried out to investigate the effect of the diffuser angle (yaw angle) on static pressure [7][12]. In addition, it investigates the value of the correlation coefficient of pressure from the inlet to the diffuser outlet. Another method to analyze the fluid flow in the ducted turbine is by using the disk actuators theory approach developed by Betz and others [8][13], where the main feature of the flow plane is the flow tube which separates the flow that passes through the disk from the flow that bypassed from the disk. The flow inside and outside the ducted is assumed to be stable, incompressible and invisible. The flow is performed with limited vorticity to the ducted downstream surface [13].

Previous studies have explained that the increase in turbine power and efficiency is obtained through the studies of the power coefficient, thrust, resistance coefficient, and axial induction factor and changing the shape and size of the turbine [4]. These parameters are very dependent on the flow velocity profile through the ducted turbine. For a certain free flow velocity, the shape and size are determined by flow velocity in the duct. Reduction of the channel cross-section accelerates the flow through the rotor plane, reducing rotor thrust loading [14].

The mass conservation equation was used to calculate the width of the stream-tube, which is increased with Reynolds number. Therefore, it will produce a higher mass-flow

from an upstream position passed through the duct throat [15].

The shape and size of the main parts of the ducted turbine determine the flow through the turbine cross-section. The duct has three important dimensions: the inlet, the diameter of the impeller housing or ducted throat, and the outlet diameter. In studies with CFD, it was found that duct applications for various duct configurations have a significant amplification of flow velocity [9]. These studies, however, have not described the flow profile in each spanwise. Therefore, it is important to calculate duct sizes precisely hence it will provide a flow profile that enhances efficiency and contributes to impeller design. Therefore, to optimize the effect of ducted shape on turbine energy parameters, it is necessary to investigate and analyze the flow characteristics in various cases of ducted turbine shape.

This study investigates the average speed and pressure in the turbine based on the velocity and pressure profiles of the flow passing through the meridional cross-section of the ducted turbine. The study is similar to the ones of Well [7] and Elshahaby [5]. In this study, five cases of the shape and geometry of ducted turbines [14] with fixed inlet and outlet diameters are investigated with flow characteristics of constant free flow speed at $U_0 = 1.5$ m/s. A similar study was also carried out by analyzing the flow by variations in the angle of attack of the ducted turbine profil [14].

This study also illustrates that the average velocity and pressure and discharge coefficients in the impeller area are theoretically obtained by using the potential flow theory [16] and the approach of flow around the body and experimental measurements [17] on each turbine section. Furthermore, flow velocity in the ducted is analyzed for turbulent flow with a commonly used factor of $1/7^{\text{th}}$ of power law [7] and uses continuance and Bernoulli principles [8] and actuator disc model [18].

The change of velocity and pressure profiles inside the duct turbine determines the performance of the turbine. Hence, this study aims to investigate the ducted turbine performance based on the effect of velocity and pressure variation resulting from shape and size modifications.

METHOD

Power Density and Turbine Geometry

The peak power of the turbine determines by the momentum theory described by Fraenkel equation [18][19]. The ocean current velocity at

the Haya Strait site reaches 2.5 m/s, with power density reaches 3755 W/m² [20]. The water flow velocity, power density data, and power requirements generated by the fluid determine the turbine's dimensions and geometry by using the continuity principle. The turbine geometry shape in this research was calculated and constructed in earlier studies [21].

The velocity profile in the ducted structure

The specific energy of the flow in the turbine duct is expressed by (1).

$$E = gH$$

$$E = \frac{1}{\rho}(p_1 - p_2) + \frac{1}{2}(v_1^2 - v_2^2) + g \cdot (z_1 - z_2) \quad (1)$$

For this condition, $p_1 = p_2$ and $z_1 = z_2$, so the specific energy equation becomes (2).

$$E = gH = \frac{1}{2}(v_1^2 - v_2^2) \quad (2)$$

The flow velocity profile that passes through the cross-section is analyzed using the turbulent flow approach. The velocity distribution at each distance of r of the ducted structure is expressed as a 1/7th power law, where the elemental velocity can be written as [7][8].

$$\frac{v}{U_o} = \left(\frac{r}{R}\right)^{1/7} \quad (3)$$

In all five-turbine cases, the shape and size of the shroud and hub sections determine the flow angle from the inlet to the outlet section. The flow direction in the ducted turbine is formulated through the potential flow theory in the duct. 1D flow analysis in the x-direction in front of the turbine uses the theory of potential flow functions for uniform flow and flow around the hub and shroud, as shown in Figure 1. The uniform flow $\psi_1 = uy = u_o r \sin \theta$ and for flow at $\psi_2 = q\theta/2\pi$ of flow source and $\psi_2 = -q\theta/2\pi$ for a sink. The superposition of uniform flow in the x-direction at the front (source) at the origin is expressed as (4).

$$\psi = \psi_1 + \psi_2 \quad (4)$$

The speed at the turbine cross-section is expressed by (5).

$$V_x = \frac{d\psi}{dy} \quad (5)$$

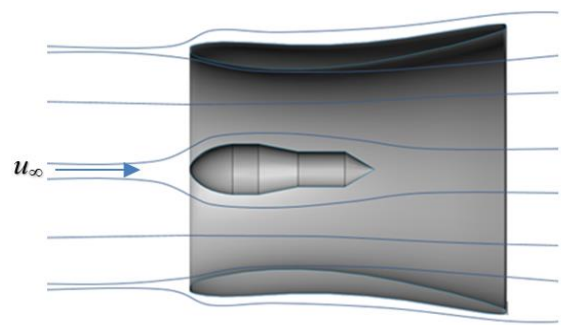


Figure 1. The contour of potential flow in the duct section

The slope angle between the velocity resultant on the flow line at each radius r is expressed as α . The velocity in the x-direction at each distance $y = r_i$, which is determined by the theory of flow around the body which is expressed as:

$$v_{ri} = v_t \cos \alpha_i \quad (8)$$

Performance Coefficient

The average speed and pressure on each turbine section are calculated by using:

$$V = \sum_{i=1}^n v_{ri}/n \quad (7)$$

The Bernoulli equation calculates the pressure at each point in the turbine by using:

$$P_{ri} = Pa + 0.5\rho v_{ri}^2 \quad (8)$$

The average velocity and pressure on each turbine cross-section are calculated by using:

$$P = \sum_{i=1}^n P_{ri}/n \quad (9)$$

Equations (6) and (8) describe the flow velocity and pressure distributions at each turbine cross-section which its radius is expressed as the relationship between the speed and pressure to y/R (p, V_x) = $f(y/R)$ for each turbine case.

The average pressure and velocity values at the inlet section is determined by the discharge coefficient value, where the discharge coefficient can be written as:

$$C_Q = \frac{V \cdot A_o}{U_o \cdot A_o} = \frac{V}{U_o} \quad (10)$$

where U_o and V are the free flow velocity and average velocity in the inlet section, respectively.

System Design

In this research, a design study and testing of a ducted turbine model was conducted at the Haya Strait site in 2015, where a ducted turbine model was used [1]. For flow measurement at each section of the turbine section, the testing stand was assembled, as shown in Figure 2.

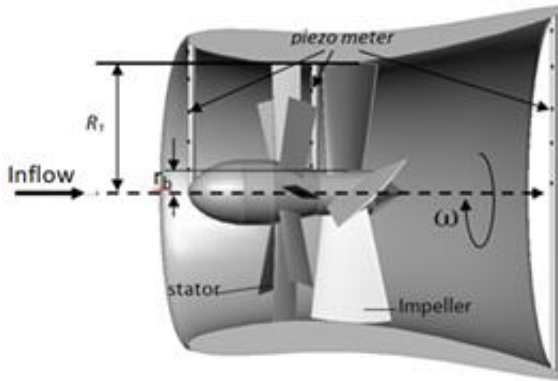


Figure 2. Turbine assembly

The water flow enters the turbine through the inlet cross-section with a fixed diameter of $D_0 = 4.0\text{m}$ to the stator and impeller with a bulb diameter of $d_b = 0.6\text{m}$. The flow exits the outlet cross-section at a diameter of $D_2 = 4.8\text{m}$. Measurements of flow velocity and pressure were carried out at a free flow velocity of $U_0 = 1.5\text{ m/s}$.

The model turbine is varied into 5 cases with different shapes and sizes to investigate the flow in the turbine. The situation is shown in Figure 3, and each model employs a diameter ratio of $\bar{d} = D_1/D_2$ [14].

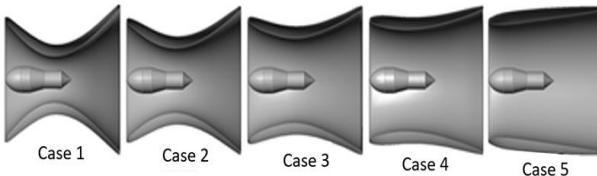


Figure 3. Five cases of turbine shape and size

The ducted data of five turbines geometry and size are shown in Table 1.

Table 1. The size of turbine geometries

No	Impeller Diameter D/D_1 (m)	Diameter Ratio $d_{bs}=D1/Do$	Angle		
			α_1	β_1	β_2
1	1.5	0.37			
2	2.0	0.49			
3	2.5	0.61	75	33.5	35
4	3.0	0.73			
5	3.5	0.85			

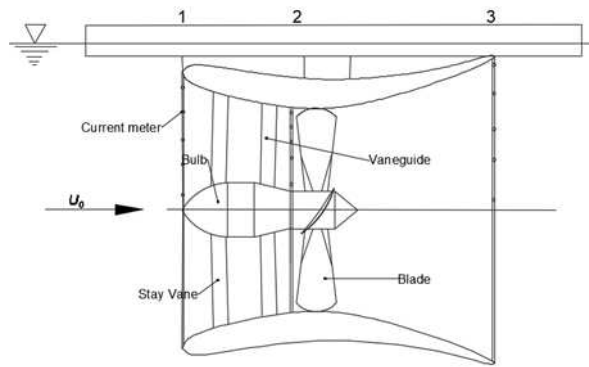


Figure 4. Testing Platform Schematic

The flow parameters that pass through the turbine section are measured at each cross-section by a current meter set up at each cross-section [6][22], as shown in Figure 4. The flow characteristic is measured at the inlet cross-sections A_0 , the impeller house A_1 , and the outlet diffuser cross-sections A_2 . The turbine measurement points are schematically shown in Figure 4. One dimensional flow velocity in the x-direction at each range of $0 \leq r \leq R$ is described as the velocity profile. Furthermore, the pressure distributions at each range are calculated using (8). The average speed and pressure values at the inlet, impeller housing, an outlet cross-section of the turbine are calculated using (7) and (9).

RESULTS AND DISCUSSION

The analysis of velocity and pressure values at each section is discussed base on the data of half of the meridian sections in the inlet area, the impeller housing or duct throat, and the outlet.

Flow Velocity and Pressure Profiles at The Inlet Cross-Section

Based on the 1D velocity value in the x-axis direction at the range $0 \leq r_1/R \leq R$ the inlet cross-section illustrates the velocity and pressure profile for the five cases shown in Figure 4. Figure 5 shows that the flow velocity $0 \leq r_1/R \leq 0.2$ tends to be fixed. At the same time, $0 \leq r_1/R \leq 1$ changes influence the condition of flow velocity in the reduction of the cross-section of the meridians in the impeller house. The results of these theoretical and experimental calculations show that the value of flow velocity of 1D in the x-direction is getting smaller by decreasing the impeller area.

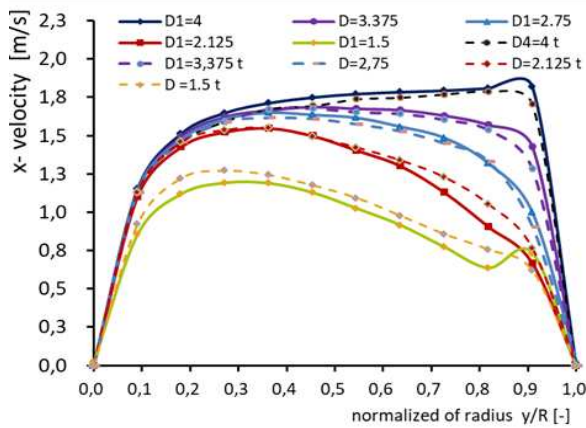


Figure 5. Velocity profiles at inlet cross-section

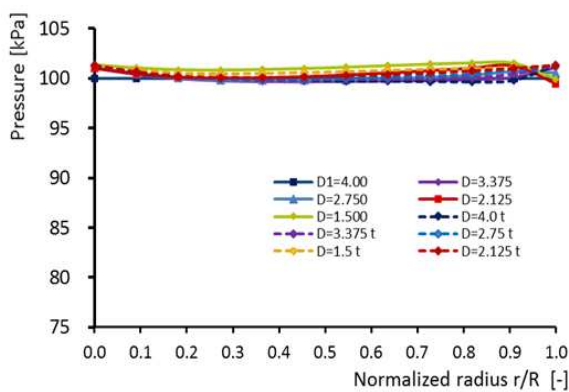


Figure 6. Pressure profiles at inlet cross-section

In a small duct throat diameter, the flow velocity at the inlet will be lower. Hence the mass-flow rate in the turbine will decrease. On the contrary, in a large section, the inlet flow speed is higher and the mass-flow rate in the turbine will be increased. Therefore, the changes in the speed profile will also change the mass-flow rate in the turbine cross-section.

The pressure on the inlet side for each change in impeller diameter D_1 , is illustrated in Figure 6. Based on (5), the inlet pressure changes after narrowing the diameter cross-section area's shape and the speed variations in the inlet.

At diameter $D_1 = D_0$, the pressure distribution at the same inclination is overall is within range of $0 < r / R \leq 1$. It is subsequently increased after the decrease in speed according to the reduction of the cross-section at the impeller house.

A similar phenomenon occurs to the velocity curve, a change in the diameter of the impeller housing or duct throat causes a change in the pressure profile in the area between the hub and shroud.

An important point on the velocity and pressure are shown in graphs of Figure 5 and Figure 6. It is shown that the size of the impeller housing diameter affects the velocity and pressure conditions in the inlet area and affects the amount of mass-flow rate that passes through the turbine.

Flow Velocity and Pressure Profiles at The Impeller House Cross-Section

The flow through the cross-section of the impeller housing is fully developed into a turbulent flow. Figure 7 shows the velocity and pressure distributions of fluid flow at the impeller house area based on semi-empirical and the range of experimental data.

According to the flow in the closed channel analysis, the maximum speed occurs in the central cross-section. The flow velocities near the periphery are higher than the flow velocities in the hub area. Likewise, the pressure on the impeller shroud area is lower than the pressure on the hub area. This phenomenon shows that the shape of the shroud and turbine hub influences the flow characteristics of the turbine.

The increase in maximum speed at each impeller diameter D_1 , compared to the speed at $D_1 = D_0$ reaches $\Delta v = 0.415, 1.097, 1.953$ and 2.02 m/s, concerning the condition where $D_1 = D_0$. At this point, the pressure difference for each case is $\Delta p = 600, 2800, 5200$ and 10500 kPa. The change in speed at each change of the impeller house cross-section area is in accordance with the Bernoulli equation's continuity principle. At $D_1 = 4$ meters, the pressure value in this area is approximately close to the pressure value at the inlet section, which is equal to $P = 100$ kPa.

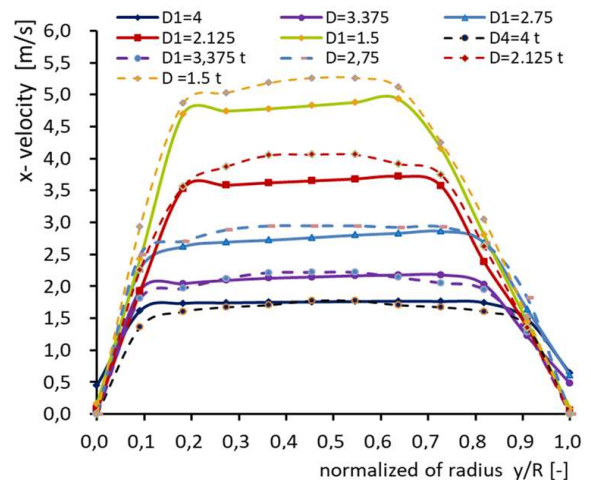


Figure 7. Velocity profiles at the impeller house cross-section

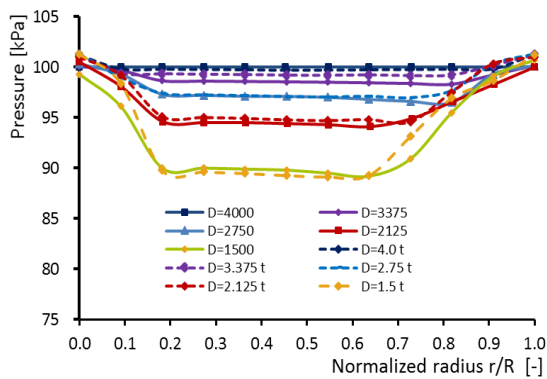


Figure 8. Pressure profiles at the impeller house cross-section

The pressure value on the inlet side for each change of the impeller diameter D_1 , is illustrated in Figure 8. Based on (5), the inlet pressure changes after the area reduction of the diameter cross-section and according to the inlet speed variation conditions. At diameter $D_1 = D_0$, the pressure distribution at the same inclination is the overall range of $0/r/R \leq 1$, subsequent condition occurs where there is a small increase of pressure and the decrease in speed when the cross-section area at the impeller occurs house is reduced.

In reverse to the conditions at the inlet, the flow velocity through the impeller housing section is higher if the cross-section is reduced. The maximum flow rate is distributed over a span of 0.15 to 0.65 for the smallest diameter (Figure 7). The reduction of the diameter of the impeller housing significantly increases the speed at the turbine cross-section. The opposite occurs in the pressure distribution graph (Figure 8), thereby reducing the diameter of the impeller housing. The pressure in this area will be smaller hence the difference between the inlet pressure and the pressure in the turbine will be higher. The increased speed of the duct throat greatly contributes to the importance of the turbine operation.

Flow Velocity and Pressure Profiles Section at The Outlet Cross-Section

Changes in shape by the reduction in diameter of the cross-section area of the impeller house have an impact on changes in flow patterns, vortices and formed wake and non-uniform flow that changes the contours of the velocity distribution and pressure on the cross-section of the outlet (Figure 9 and Figure 10). At a diameter ratio of 0.83 and 0.73, the velocity distribution along the data range shows a nearly uniform flow pattern.

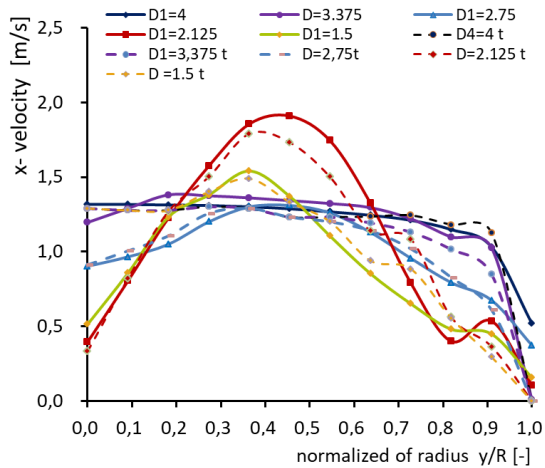


Figure 9 Velocity profile of the outlet cross-section

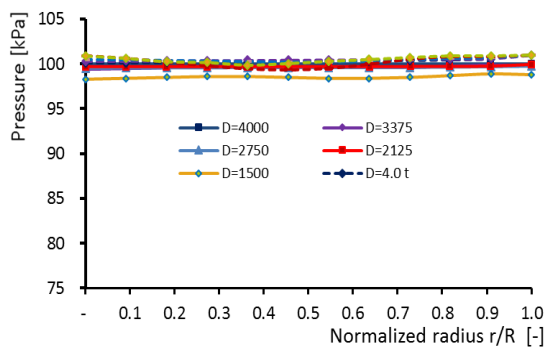


Figure 10. Pressure profile of the outlet cross-section

Vortex and wake start to form when the diameter ratio is equal to 1 and increases at a diameter ratio of 0.49 to 0.37. The flow velocity on the x-axis is greater for the small diameter of the impeller housing. In contrast, at the larger diameter (D_1 approaches D_0), the flow velocity in the x-direction at the outlet reaches a minimum value according to the principle of continuity. Flow velocity in $0.3 \leq r/R \leq 0.6$ reaches the minimum value in the area near the axis and shroud.

In contrast to the conditions at the inlet, the reduction of the cross-section, the flow velocity profile through the outlet section of the outlet flow velocity produces a non-uniform condition (Figure 9). Still, it does not have a significant effect on static pressure.

Average Speed and Pressure on Ducted Sections

The average speed and pressure values for each cross-section in the five ducted cases are depicted in Figure 11 and Figure 12. The figure shows the change in average velocity and pressure on each cross section of the ducted

turbine. At fixed inlet and outlet diameters, the size of the impeller diameter affects the flow at the front and behind the turbine. The smaller the impeller diameter, the smaller fluid velocity at the inlet and the outlet cross-section, while the greater fluid velocity in the impeller area. The opposite condition occurs for greater pressure at low speeds at the inlet and outlet, and it is smaller at high speeds at small impeller houses. The distribution of average velocity and pressure in the third inlet area of the turbine section of the five turbine cases is shown in Figure 7.

Figure 11 and Figure 12 show that by reducing the diameter of the impeller housing, the average velocity at the meridian section is higher and the pressure is lower. The increase in flow velocity and the pressure at the inlet cross-section and the impeller housing will determine the head, power, and turbine rotational speed values. These parameters become important data in turbine design. The high-speed flow in the internal duct increases the available head, hydraulic power, and turbine rotational speed.

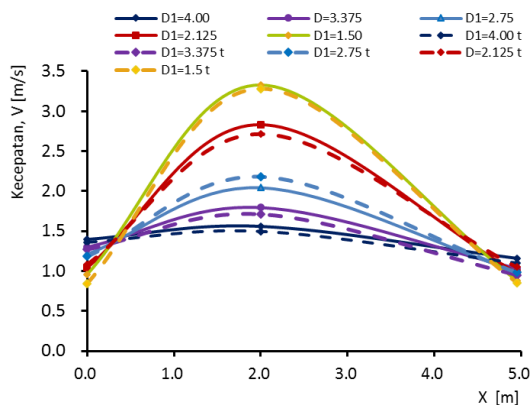


Figure 11. Average velocity for the five ducted cases

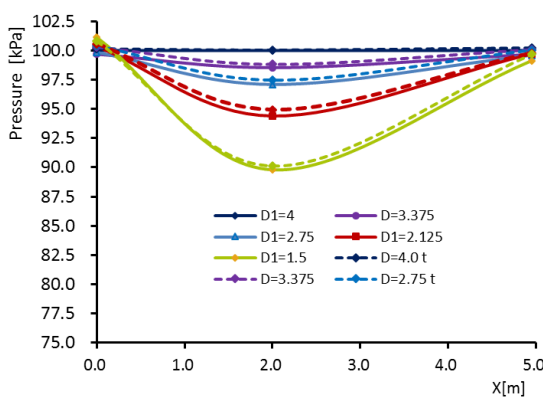


Figure 12. Average pressure for the five ducted cases

Effect of Impeller Diameter on Flow Energy Parameters in Ducted.

Figure 13 shows that the change in Impeller diameter D_1 affects the flow pattern in the ducted turbine, even though the free flow velocity in front of the cross section $V_0 = \text{constant}$. The average speed at the turbine inlet for all five turbine cases ranges from 0.94 to 1.4 m/s. Figure 13 shows that the average value of velocity at the inlet section slows down following the reduction in impeller diameter D_1 in the same inlet size, thereby reducing the discharge coefficient C_Q value.

Conversely, the static pressure value at the inlet section is higher for smaller D_1 diameters. In accordance with Betz's theory, at higher inlet pressures, a portion of the fluid will flow through the outside of the inlet section. The smaller the impeller house's cross section, the increasing volume of fluid will not pass through the duct. This is in accordance with the continuity equation. The inlet cross-section area A_0 and free speed $V_0 = \text{constant}$. Therefore, the C_Q discharge coefficient value is only influenced by the shape and size of the impeller house diameter. In this study, the C_Q values of the turbine section ranged from 0.64 to 0.93 (Figure 8).

In an analogy to the research conducted by Borg et al. [12]. The results of the velocity profile analysis show that the internal flow velocity is accelerating through a reduction in the diameter of the duct throat (impeller area). Also, the maximum axial flow velocity in the plane between the hub and shroud exceeds the free speed. This is because the point of maximum axial velocity is located around the center of spanwise. This axial velocity is then reduced outside the orifice region due to channel enlargement.

The velocity profile in the impeller or duct throat area is in accordance with the numerical simulation of the Diffuser of a gas turbine using the actuator disc model conducted by Sadasivan et al. [23].

In line with shape design research with CFD analysis conducted by Jo et al. [9], the flow velocities inside were increased one of the smaller duct throat diameters than the inlet diameter. Therefore, the duct performance has been enhanced significantly by the modification.

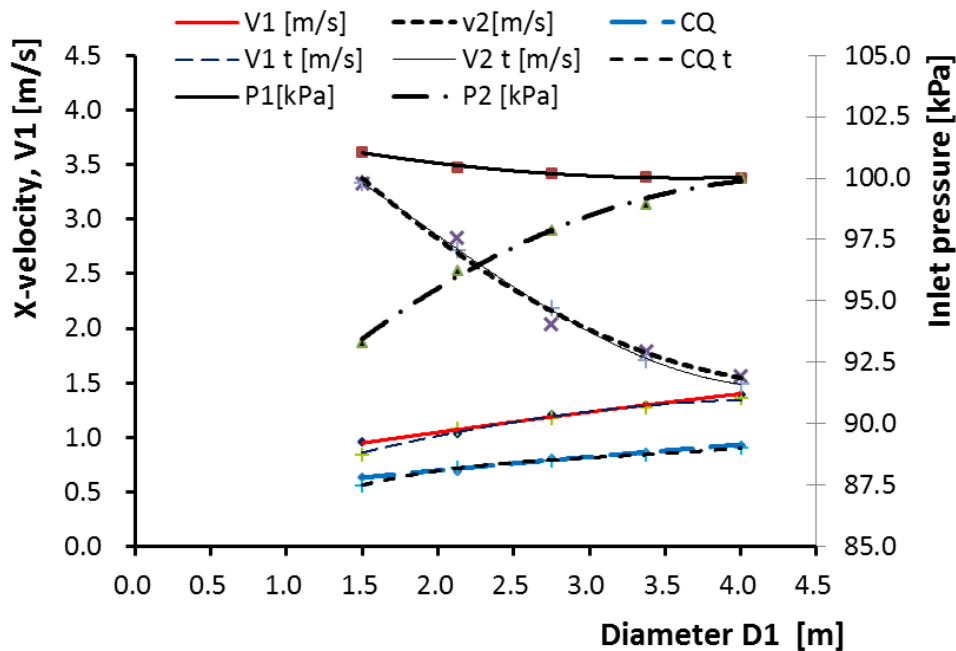


Figure 13. Effect of changes in impeller diameter in velocity, pressure and coefficient of discharge (V, P, C_Q) = $f(D_1)$ on the inlet and impeller sides

Similar to the study of NACA 0015 for diffuser design in tidal current turbine applications conducted by Mehmooda et al. [10]. The enlargement of the attack angle means that the outlet diameter increases with a fixed diameter of the impeller area or duct throat at a fixed outlet diameter, meaning that the inlet diameter is small. This change increases the maximum speed from 1.5÷3.18 m/s or 1.25÷2.65 times the freestream velocity. In this study, to reduce the diameter ratio from $dr = 1-0.375$, the velocity at the section between the hub and shroud in the duct throat was 1.15÷2.21 times the freestream velocity.

However, the discharge coefficient or mass flow rate decreased slightly in the small impeller diameter in this study. Increased flow velocity in the duct will increase the values of important parameters, namely the amplification value of the factor [9], the coefficient of velocity and pressure, and increasing the power coefficient and thrust coefficient [10, 11, 14]. The power coefficient is relevant to the absolute size of a turbine [24]. The maximum value of the power coefficient was determined at $dr = 0.61\div 0.73$ or $dr = 0.69$ [14] that is equivalent to the average internal flow velocity $V_r = 2.0\div 2.6$ m/s and the static pressure 97.1÷ 94.4 kPa.

Figure 13 shows that the flow velocity is higher in a small duct throat diameter but decreases the discharge coefficient. The value of

velocity, pressure, and flow rate through the turbine is important information in turbine design. These parameters are dependent on the shape and size of the turbine ducted. Thus, the optimal turbine construction is determined based on the analysis result of these parameters.

CONCLUSION

Theoretical calculation and experimental case study show that x-axis flow velocity at throat diameter inlet and outlet is constant for $D_0/D_2 = 0.83$. On the other hand, the reduction of throat diameter D_1 increases internal flow velocity, hence the axial speed at the cross section of the impeller housing. In this case, the velocity at the throat section is higher than the one in the duct inlet section. Flow velocity at impeller area increased from 1.76 to 4.8, which corresponds to $dr = 1$ to $dr = 0,37$, while static pressure decreased. Thus, the increase of velocity and decrease of static pressure affected the decrease of debit coefficient in which it decreased from $C_Q = 0,9$ in $dr = 1$ to $C_Q = 0,56$ at $dr = 0,37$.

This case shows that in determining the optimal diameter value, an optimization process of the shape and size of the duct turbine is needed. The increase of velocity and decrease of pressure produces a significant effect on turbine performance, represented by power and thrust coefficients. Hence, the value at $D_0/D_2 = 0.83$, ratio of optimal diameter $dr_{opt} = 0,61\div 0.73$ or dr_{opt}

= 0,69 [14]. That is equivalent to average internal flow velocity $V_r = 2.0 \div 2.6$ m/s and the static pressure of $p_s = 97.1 \div 94.4$ kPa. These values are related to the duct model of case 3 and case 4, but leaning more towards case 4. In this case, the velocity of the throat diameter section reaches 2.21 times greater than the inlet velocity value. The shape and size modification of the cross section of impeller housing produce a maximum power coefficient related to the shape and optimal size of the duct turbine.

REFERENCES

- [1] W. M. Rumaherang, R. Ufie, J. Louhenapessy and J. Latuny, "Karakteristik Turbin Propeller Sumbu Horizontal Pembangkit Listrik Tenaga Arus Laut," in *Prosiding Archipelago Engineering ALE 2018*, Ambon, Indonesia, 2018, pp. 90–95
- [2] J. M. Laurens, M. Ait, Mahrez and M. Tarfaoui, M, "Design of bare and ducted axial marine current turbines," *Renewable Energy*, vol. 89, pp. 181-187, April 2016, doi: 10.1016/j.renene.2015.11.075
- [3] A. Roberts, B. Thomas, P. Sewell, Z. Khan, S. Balmain, and J. Gillman, "Current tidal power technologies and their suitability for applications in coastal and marine areas," *Journal of Ocean Engineering and Marine Energy*, vol. 2, no. 2, pp. 227–245, 2016, doi: 10.1007/s40722-016-0044-8
- [4] M. Shives and C. Crawford, "Developing an empirical model for ducted tidal turbine performance using numerical simulation results," *Proceeding of the Institution of Mechanical Engineers Part A, Journal of Power Energy*, vol. 226, no. 1, pp. 112–125, 2012, doi: 10.1177/0957650911417958
- [5] A. M. El-Zahaby, A. E. Kabeel, S. S. Elsayed, and M. F. Obiaa, "CFD analysis of flow fields for shrouded wind turbine's diffuser model with different flange angles," *Alexandria Eng. J.*, vol. 56, no. 1, pp. 171–179, 2017, doi: 10.1016/j.aej.2016.08.036
- [6] T. A. Khamlaj and M. P. Rumpfkeil, "Theoretical analysis of shrouded horizontal axis wind turbines," *Energies*, vol. 10, no. 1, 2017, doi: 10.3390/en10010038
- [7] N. W. Cresswell, G. L. Ingram, and R. G. Dominy, "The impact of diffuser augmentation on a tidal stream turbine," *Ocean Engineering*, vol. 108, pp. 155–163, 2015, doi: 10.1016/j.oceaneng.2015.07.033
- [8] S. Allsop, C. Peyrard, P. R. Thies, E. Boulougouris, and G. P. Harrison, "Hydrodynamic analysis of a ducted, open centre tidal stream turbine using blade element momentum theory," *Ocean Engineering*, vol. 141, no. January, pp. 531–542, 2017, doi: 10.1016/j.oceaneng.2017.06.040
- [9] C. H. Jo, D. Y. Kim, S. J. Hwang, and C. H. Goo, "Shape design of the duct for tidal converters using both numerical and experimental approaches (pre-2015)," *Energies*, vol. 9, no. 3, 2016, doi: 10.3390/en9030185
- [10] N. Mehmood, "Study of NACA 0015 for Diffuser Design in Tidal Current Turbine Applications," *International Journal of Engineering*, vol. 25, no. 4(C), pp. 373–380, 2012, doi: 10.5829/idosi.ije.2012.25.04c.12
- [11] M. Maduka and C. W. Li, "Numerical study of ducted turbines in bi-directional tidal flows," *Engineering Application of Computational Fluid Mechanics*, vol. 15, no. 1, pp. 194–209, 2021, doi: 10.1080/19942060.2021.1872706
- [12] M. G. Borg, Q. Xiao, S. Allsop, A. Incecik, and C. Peyrard, "A numerical swallowing-capacity analysis of a vacant, cylindrical, bi-directional tidal turbine duct in aligned & yawed flow conditions," *Journal of Marine Science and Engineering*, vol. 9, no. 2, pp. 1–22, 2021, doi: 10.3390/jmse9020182
- [13] S. Draper and T. Nishino, "Centred and staggered arrangements of tidal turbines," *Journal of Fluid Mechanics*, vol. 739, no. March, pp. 72–93, 2014, doi: 10.1017/jfm.2013.593
- [14] W. M. Rumaherang, "The effect of diameter ratio on energy parameters of the tidal turbine tidal turbine," *Dinamika Teknik Mesin*, vol. 10, no. 1, p. 1, 2020, doi: 10.29303/dtm.v10i1.306
- [15] D. Sakagucchi and Y. Kyozuka, "Design of A Shrouded Tidal Current Turbine by Multi-Objective Optimization," *Grand Renewable Energy 2018 Proceedings*, Yokohama, Japan, June 2018, vol. 17, pp. 4–7
- [16] Md. S. Tarafder and N. Nabila, "Analysis of potential flow around two-dimensional body by finite element method," *Journal of Mechanical Engineering Research*, vol. 7, no. 2, pp. 9–22, 2015, doi: 10.5897/jmer2014.0342
- [17] M. Edmunds, A. J. Williams, I. Masters, A. Banerjee, and J. H. VanZwieten, "A spatially nonlinear generalised actuator disk model for the simulation of horizontal axis wind and tidal turbines," *Energy*, vol. 194, p. 116803, 2020, doi: 10.1016/j.energy.2019.116803
- [18] T. A. Theoyana, Purwanto, W. S. Pranowo, "Potensi Energi Arus Laut Pada Berbagai Kedalaman Untuk Jurnal Oseanografi," *Journal of Oceanography*, vol. 4, no. 1, pp.

- 262–269, 2015
- [19] K. Orhan and R. Mayerle, “Assessment of the tidal stream power potential and impacts of tidal current turbines in the Strait of Larantuka, Indonesia,” *Energy Procedia*, no. 125, pp. 230–239, 2017
- [20] W. M. Rumaherang, R. Ufie, J. Louhenapessy, and J. Latuny, “Design and Evaluation of Energy Characteristics of a Horizontal Venturi Bulb Turbine Based on Sea Current Data of The Haya Strait,” *Prosiding SNTTM XVII*, Indonesia 2018, pp. 88–92
- [21] W. M. Rumaherang, R. Ufie and J. Latuny, “Optimization of Output Parameters of The Horizontal Tidal Turbine by Modifying Its Meridional Section,” 2018 2nd Borneo International Conference on Applied Mathematics and Engineering (BICAME), 2018, pp. 18-22, doi: 10.1109/BICAME45512.2018.1570498954
- [22] R. A. Chihaiia, L. A. El-Leathey, G. Cîrciumaru, and N. Tănase, “Increasing the energy conversion efficiency for shrouded hydrokinetic turbines using experimental analysis on a scale model,” *E3S Web Conf.*, vol. 85, pp. 0–5, 2019, doi: 10.1051/e3sconf/20198506004
- [23] S. Sadasivan, S. K. Arumugam, and M. C. Aggarwal, “Numerical simulation of diffuser of a gas turbine using the actuator disc model,” *Journal of Applied Fluid Mechanics*, vol. 12, no. 1, pp. 77–84, 2019, doi: 10.29252/jafm.75.253.28416
- [24] L. Y. Chang, F. Chen, and K. T. Tseng, “Dynamics of a marine turbine for deep ocean currents,” *Journal of Marine Science and Engineering*, vol. 4, no. 3, 2016, doi: 10.3390/jmse4030059